



in the new design, but can be small enough that it does not significantly increase the beam divergence. Part of the horizontal chromaticity must be generated upstream of the bend in order to cancel the second order dispersion.

The third order geometric aberrations generated by the sextupoles are:  $U_{1222} = K_{SD}K_{SF}R_{D12}^2R_{F12}^2\psi_{12}$

$$U_{3444} = K_{SD}K_{SF}R_{D34}^2R_{F34}^2\psi_{12}$$

$$U_{1244} = U_{3224} = -K_{SD}K_{SF}[\psi_{12}R_{D34}^2R_{F12}^2 + \psi_{12}R_{D12}^2R_{F34}^2 - 4\psi_{34}R_{D12}R_{D34}R_{F12}R_{F34}]/2$$

where  $\psi_{12}$  and  $\psi_{34}$  are elements of transfer matrix between  $S_{F1}$  and  $S_{D1}$ . The term  $U_{3444}$  is small if the last quadrupole is defocusing.  $U_{1222}$  is negligible for typical parameters of flat beams.  $U_{1244}$  and  $U_{3224}$  can be made to vanish. Similar constraints hold for third order chromo-geometric aberrations. All these constraints can be satisfied with the simple system described above. A system with the same demagnification as the NLC FF and comparable optical performance can be built in a length of about 300 m.

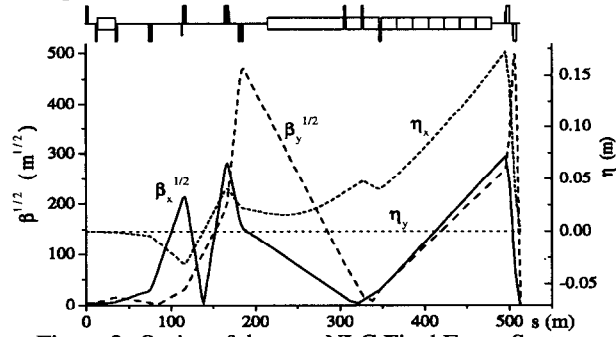


Figure 3: Optics of the new NLC Final Focus System.

### 3 PERFORMANCE OF THE NEW FF

The new FF system has potentially much better performance than the traditional design. The “minimal” optics concept can be further improved by adding more elements to minimize residual aberrations. An additional bend upstream of the second sextupole pair decreases chromaticity through the system. An additional sextupole upstream and in phase with the last one further reduces aberrations in x-plane. Since such system is “ideal” up to third order, additional decapoles can give further improvements. The new optics is shown in Fig.3. The flat beam parameters are given in Table 1. The new system has an  $L^* = 4.3$  m, which is twice the original value. This allows the use of large bore superconducting quadrupoles and simplifies the design of the detector. Although the chromaticity is doubled due to the larger  $L^*$ , the performance of the system is still better than for the original NLC FF design.

Table 1: Beam parameters

|   |            |
|---|------------|
| Beam energy, GeV  | 500        |
| Normalized emittances $\gamma\epsilon_x / \gamma\epsilon_y$ ( $\mu\text{m}$ ) | 4 / 0.06   |
| Beta-functions $\beta_x / \beta_y$ at IP (mm)                                 | 9.5 / 0.12 |
| Beam sizes $\sigma_x / \sigma_y$ at IP (nm)                                   | 197 / 2.7  |
| Beam divergence $\theta_x / \theta_y$ at IP ( $\mu\text{rad}$ )               | 21/23      |
| Energy spread $\sigma_E$ ( $10^{-3}$ )  | 3          |
| Dispersion' $\eta'_x$ at IP ( $10^{-3}$ )                                     | 5.4        |

Figs.4,5,6 compare the bandwidth of the NLC FF and the new design. Figs.4,5 show the IP beamsize as a function of energy and the luminosity reduction as a function of energy spread. Beam size and luminosity in Fig.5 were improved with two additional decapoles. Fig.6 shows the bandwidth in terms of the beamsize at the final doublet. The bandwidth is derived from the variation of the beta function and the beam sizes as they actually contribute to luminosity, which is determined by tracking. The beam size bandwidth is narrower than the beta function bandwidth because of higher order cross-plane chromatic aberrations. While the IP bandwidth for these two systems is comparable, the FD bandwidth is much wider for the new FF.

Fig.7 shows the halo particle distribution at the face of the final doublet for the traditional FF and for the new FF. The beam is very distorted in the traditional FF while the nonlinear terms are still negligible for the new FF. The nonzero dispersion across the FD in the new system has little affect on the dynamic aperture. In addition, the design aperture of the NLC final doublet is about  $r_a = 10$  mm while for the new FF with twice longer  $L^*$  this aperture can be as large as  $r_a = 40$  mm. Therefore the collimation requirements for the new FF may be relaxed by a factor of at least one hundred in the IP phase, and by a factor of at least 3 for the FD phase and energy without increasing particle losses at the FD.

Due to the shorter length of the system, there would also be less regeneration of the beam halo in the final focus itself from beam-gas scattering, reducing an additional source of background.

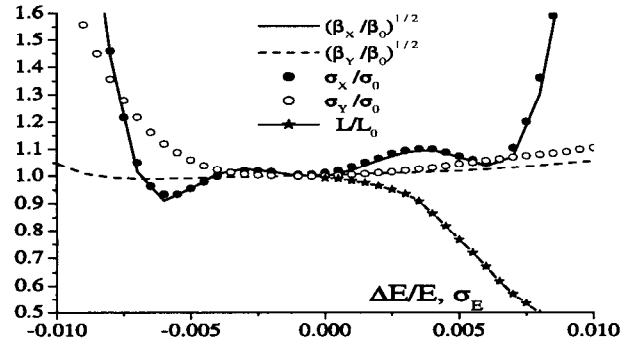


Figure 4: IP bandwidth of the traditional NLC Final Focus. Normalized betatron functions and normalized luminosity equivalent beam size versus energy offset  $\Delta E/E$ , and normalized luminosity versus rms energy spread  $\sigma_E$ .

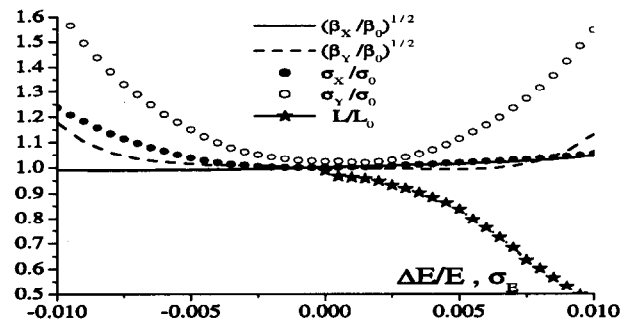


Figure 5: IP bandwidth of the New NLC Final Focus.

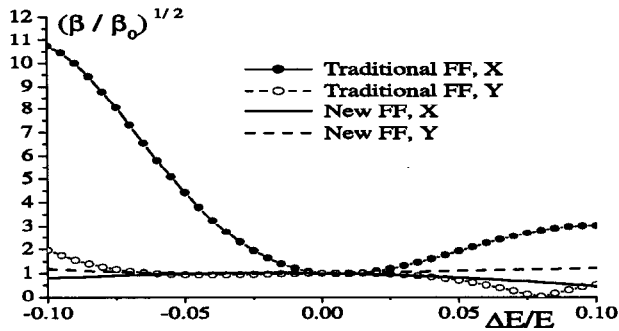


Figure 6: FD bandwidth of the Traditional and New NLC Final Focus. Normalized betatron functions at the final doublet versus energy offset  $\Delta E/E$ .

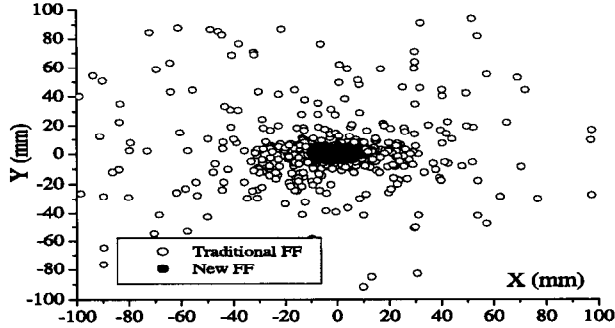


Figure 7: Beam at the entrance of the final doublet for the traditional NLC FF and for the new FF. Particles of the incoming beam are placed on a surface of an ellipsoid with dimensions  $N_\sigma(x, x', y, y', E) = (800, 8, 4000, 40, 20)$  times larger than the nominal beam sizes.

#### 4 SCALING WITH $\epsilon$ AND ENERGY

To maintain optimal performance of the system with larger incoming beam emittances, the bend field must increase like  $B_0 \propto \sqrt{\epsilon}$ . The increased field is necessary to hold constant the contribution of high order aberrations to the IP beam size, as well as the contribution of the IP angular dispersion  $\eta'_{IP}$  to the beam divergence.

The scaling to higher energies is much easier with the new design. For a wide range of parameters, the IP spot size dilution is dominated by the energy spread created by synchrotron radiation in the bends. This scales like

$$\frac{\Delta\sigma_y}{\sigma_y} \propto \frac{\gamma^5}{L^2} \eta_B'^3 \propto (\gamma\epsilon_y)^{3/2} \left(\frac{\eta_B' L}{\eta_{IP}'}\right)^3 \left(\frac{\eta_{IP}'^2}{\epsilon_y}\right)^{3/2} \frac{\gamma^{7/2}}{L^5}$$

where  $\eta_B'$  is the angular dispersion produced by the bends where the bend length is assumed to be proportional to the total length of the system  $L$ . The terms in the parenthesis are constant if the IP angular dispersion is proportional to the beam divergence and if we conservatively assume that the normalized emittance will be the same at higher energies. In this case the length of the system scales with energy as  $L \propto \gamma^{7/10}$ . If, however, the achievable normalized emittance scales approximately inversely with energy, as is assumed in [2], then the scaling becomes  $L \propto \gamma^{2/5}$ . In this case, with the new design, the FF for a 3 TeV center of mass energy collider could be only about 700 m long.

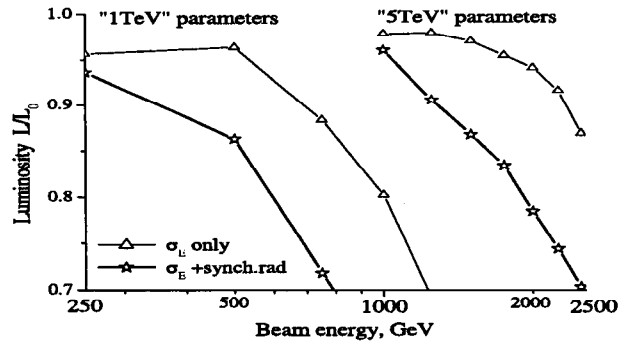


Figure 8: Luminosity vs beam energy for the new FF, bend field optimized at each energy, beam with energy spread. With and without synchrotron radiation. The “1TeV” parameters correspond to Table.1, the “5TeV” set corresponds to [2] with  $\gamma\epsilon = 50/1 \cdot 10^{-8}$  m,  $\beta^* = 9.5/0.14$  mm,  $\sigma_E = 0.2\%$  and  $\sigma^*$ (at 2.5TeV/beam)= 31/0.54 nm.

The beam also emits synchrotron radiation in the quadrupoles which becomes more of a problem at higher energies. This can be reduced in the new design because the larger bandwidth allows the FD quadrupoles to be lengthened to minimize the synchrotron radiation generated in them.

For the presented optics, the dependence of the luminosity on beam energy is shown in Fig.8. Clearly a fixed length final focus has a wide range of energies where it could operate. If the beam parameters from [2] are assumed, this FF can operate almost up to 5TeV in the center of mass.

#### 5 CONCLUSION

We have developed a new Final Focus system that has better properties than the systems so far considered and built. It is much shorter, providing a significant cost reduction for the collider. The system has similar bandwidth and several orders of magnitudes larger dynamic aperture. This reduces the backgrounds and relaxes the design of the collimation section. It is also compatible with an  $L^*$  which is twice as long as that in the traditional NLC FF design, which simplifies engineering of the Interaction Point area. Finally, its favorable scaling with beam energy makes it attractive for multi-TeV colliders.

We believe that further improvements of the performance of the system are possible.

We would like to thank N. Phinney, T. Raubenheimer and P. Tenenbaum for very useful discussions.

#### 6 REFERENCES

- [1] NLC ZDR Design Group, “A Zeroth-Order Design Report for the Next Linear Collider”, SLAC Report-474 (1996).
- [2] J.P. Delahaye, G. Guignard, J. Irwin, T.O. Raubenheimer, R.D. Ruth, I. Wilson, P.B. Wilson, “A 30 GHz 5-TeV Linear Collider”, PAC 1997 Proceedings, (1998), p.482.
- [3] P. Raimondi, A. Seryi “A novel Final Focus design for future Linear Colliders”, SLAC-PUB-8460, May 2000, submitted to Phys. Rev. Lett.